无 机 化 学 学 报

2015 年　　第 31 卷　　第 10 期

目　次

论　文

CHINESE JOURNAL OF INORGANIC CHEMISTRY

Vol.31 No.10 Oct. 2015

CONTENTS

Cover

Articles

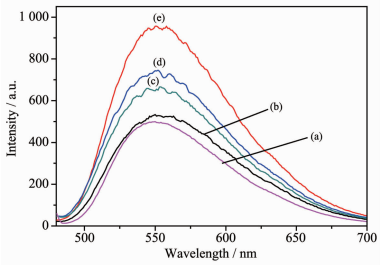

Under excitation with 470 nm blue-light, the yellow-fluorescent hydrotalcite-like composition can exhibit yellow emission at 557 nm. The fluorescence intensity of composition can be improved by modified with silane coupling agent. The hydrotalcite-like composition was successfully applied in WLED device.

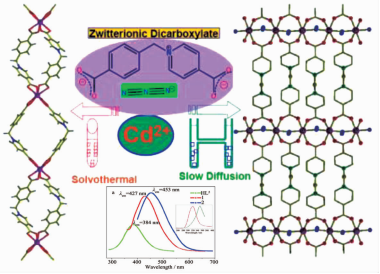

The assembly of Cd(Ⅱ) ions with newly synthesized zwitterionic dicarboxylate ligand leads to two different CPs with dimensionalities from 1D to 2D by controllable syntheses, and fluorescent measurements shows that emission bands can be correlated to the coordination modes of the L ligand.

One Step Synthesis of Fe/N Co-Doped Carbon Nanoparticles for Photocatalysis

LI Hong-Ren, ZHANG Yan, LIU Shi-Qi, LI Feng

DOI:10.11862/CJIC.2015.270
Chinese J. Inorg. Chem., **2015**,**31**:1938-1945

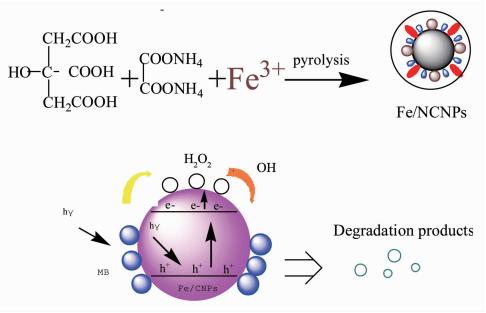

A High Selective Fluorescent Ratio Sensor for Cd^{2+} Based on the Interaction of Peptide with Metal Ion

WANG Zhao-Lu, FENG Hui-Yun, LI Yan, XU Tao, XUE Ze-Chun, LI Lian-Zhi

DOI:10.11862/CJIC.2015.261
Chinese J. Inorg. Chem., **2015**,**31**:1946-1952

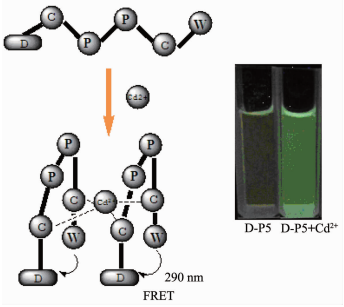

A fluorescent ratio chemosensor (Dansyl-Cys-Pro-Pro-Cys-Trp-NH_2) for Cd^{2+} has been synthesized via Fmoc solid-phase peptide synthesis. It showed highly selective and sensitive recognition toward Cd^{2+}.

Effects of Calcination Temperature on Crystal Structure and Photocatalytic Activity of In_2TiO_5 Nanobelts

ZHANG Qin-Ku, YAO Bing-Hua, YU Yan, LU Pan, PANG Bo, XIONG Min

DOI:10.11862/CJIC.2015.175
Chinese J. Inorg. Chem., **2015**,**31**:1953-1958

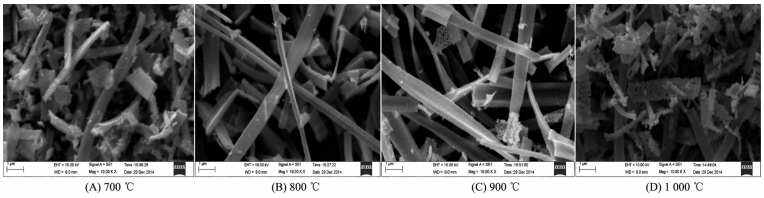

The morphology of In_2TiO_5 nanobelts significantly becomes more narrower and thinner with the increase of calcination temperature. When the calcination temperature is over 900 ℃, the In_2TiO_5 nanobelts show the morphology of nano-porous structure.

Nano-WO_3: Preparation, Characterization and Effect on Thermal Decomposition of Hexanitrohexaazaisowurtzitane

ZHAO Ning-Ning, HE Cui-Cui, WANG Tong, AN Ting, ZHAO Feng-Qi, HU Rong-Zu, MA Hai-Xia

DOI:10.11862/CJIC.2015.263
Chinese J. Inorg. Chem., **2015**,**31**:1959-1965

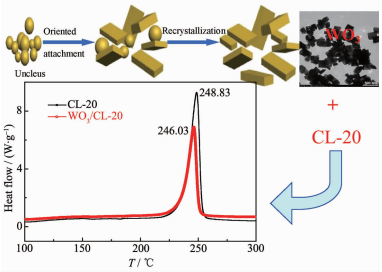

Based on the preparation of nanosized WO_3 cuboids, the effects of WO_3 cuboids on the thermal decomposition of CL-20 were investigated. WO_3 cuboids play an important role in reducing the peak temperature of the decomposition and the activation energy of CL-20.

Effect of Different Second Particle Size on Rate Capability of Li-Rich Layered Cathode Materials $Li_{1.2}Mn_{0.54}Ni_{0.13}Co_{0.13}O_2$

YIN Yan-Ping, LU Hua-Quan, WANG Zhong, SUN Xue-Yi, ZHUANG Wei-Dong, LU Shi-Gang

DOI:10.11862/CJIC.2015.271
Chinese J. Inorg. Chem., **2015**,**31**:1966-1970

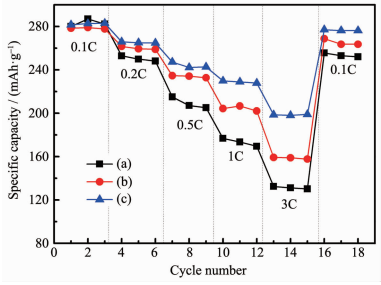

The $Li_{1.2}Mn_{0.54}Ni_{0.13}Co_{0.13}O_2$ materials with smaller second particle size showed a much superior rate capability to the sample with bigger particle size. The improvement in rate capability could be attributed to the smaller particle size, which gives a better contact between the active material and the electrolyte/conductive agent, at the same time a shorter diffusion path.

Photocatalytic Performance and Photolysis Mechanism of Ag_2S/ZnO with Visible-Light Response Prepared by Microwave Hydrothermal Two-Step Method

CHEN Xi, LI Li, ZHANG Wen-Zhi,
SONG Qiang, LI Yi-Xuan

DOI:10.11862/CJIC.2015.269
Chinese J. Inorg. Chem., **2015**,**31**:1971-1980

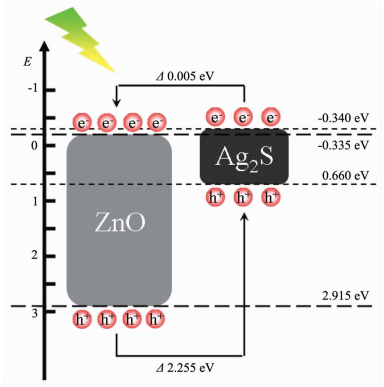

The presence of Ag_2S enhances the light absorption of the photocatalyst under the visible-light region and suppresses the growth of ZnO along the (001) crystal plane. When n_{Ag_2S}/n_{ZnO} was 1∶10, the composite performs higher photocatalytic activity than P25 widely used at present.

Cooperation Effect of Cu(Ⅱ) Cocatalyst and Graphene for Enhanced AgBr Visible-Light Photocatalytic Performance

WANG Ming-Fang, WANG Ping,
XU Shun-Qiu, LI Xiao-Zheng

DOI:10.11862/CJIC.2015.235
Chinese J. Inorg. Chem., **2015**,**31**:1981-1986

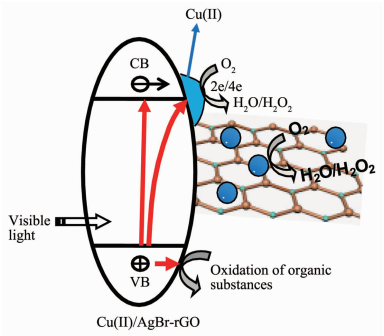

The highly efficient AgBr photocatalyst was developed with cooperation effect of Cu(Ⅱ) cocatalyst and graphene as Cu(Ⅱ) can catch electrons and graphene may provide a lot reduction active sites.

Preparation and Liver MRI of Fe_3O_4/*N*-(2-Hydroxyl)propyl-3-trimethyl Ammonium Chitosan Contrast Agent

SONG Xiao-Li, LUO Xia-Dan, LI Ling,
ZHU Ai-Ping

DOI:10.11862/CJIC.2015.230
Chinese J. Inorg. Chem., **2015**,**31**:1987-1992

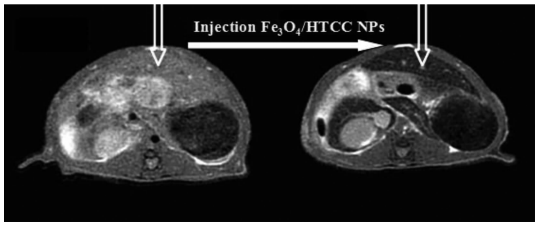

Supermagnetic Fe_3O_4/*N*-(2-hydroxyl) propyl-3-trimethyl ammonium chitosan nanoparticles with good suspension stability and cytocompatibility have potential application in liver MRI as a negative contrast.

Syntheses, Structures and Properties of Two Cadmium Complexes Constructed from a Flexible Tetrahedral Ligand

LIANG Li-Li, XU Lei, CHEN Fei-Jian,
SI You-Lin, TAO Zhao-Lin, XUE Hong-Bao

DOI:10.11862/CJIC.2015.210
Chinese J. Inorg. Chem., **2015**,**31**:1993-2000

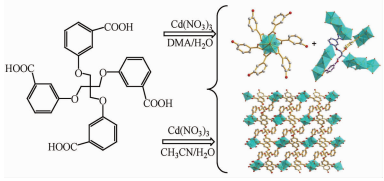

Two cadmium coordination polymers, $[Cd_6L_3(DMA)_3(H_2O)]_n$ (**1**) and $\{[Cd_2L(H_2O)_4]\cdot 4H_2O\}_n$ (**2**) (L=tetrakis[3-(carboxyphenyl)oxamethyl]methane acid) with different structures have been synthesized. In compound **1**, the tetrahedral ligand connects four Cd_3 clusters and the Cd_3 clusters connect six benzoic rings to form a 4,6-connected 3-dimentional framework of the *toc* topology. Each ligand of compound **2** connects four cadmium atoms and the cadmium atoms are connected through carboxylates to form a chain.

Syntheses, Crystal Structures and *in vitro* Anti-tumor Activity of Three Bis[tris(2-methyl-2-phenyl)propyltin] dicarboxylate $(CH_2)_n[CO_2Sn(CH_2CMe_2Ph)_3]_2$ (n=2, 3, 4)

KUANG Dai-Zhi, ZHU Xiao-Ming,
FENG Yong-Lan, ZHANG Fu-Xing,
YU Jiang-Xi, JIANG Wu-Jiu, TAN Yu-Xing,
ZHANG Zhi-Jian

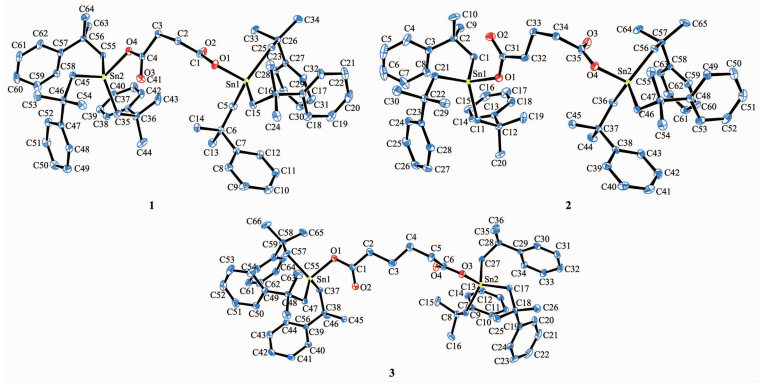

Three complexes belong to distorted tetrahedral configuration with four-coordination for the central tin atom. The complexes exhibited strong in vitro anti-tumor activity against five human tumor cell lines, Colo205, HepG2, MCF-7, Hela and NCI-H460.

DOI:10.11862/CJIC.2015.211
Chinese J. Inorg. Chem., **2015**,**31**:2001-2007

Syntheses, Crystal Structures and Magnetic Properties of Co(Ⅱ) and Mn(Ⅱ) Complexes with 4-(4-Pyridinemethyleneamino)-1,5-dimethyl-2-phenyl-1,2-dihydropyrazol-3-one

PANG Hai-Xia, YUAN Xi-Ming,
WANG Xian-Wen, HE Xiong

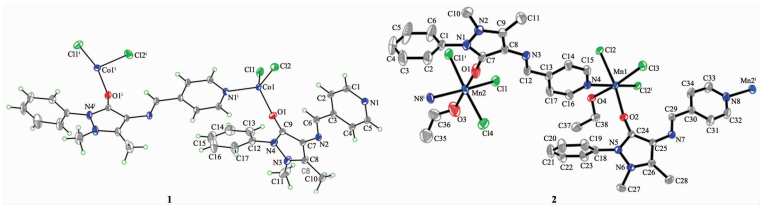

Two complexes $[CoLCl_2]$ (**1**) and $[MnLCl_2]$ (**2**) were prepared under solvo-thermal conditions with 4-(4-pyridinemethyleneamino)-1,5-dimethyl-2-phenyl-1,2-dihydropyrazol-3-one (L), $CoCl_2\cdot 6H_2O$ and $MnCl_2\cdot 4H_2O$. As the temperature drops, the two complexes show the antiferromagnetic interactions. They can be used potential magnetic materials.

DOI:10.11862/CJIC.2015.243
Chinese J. Inorg. Chem., **2015**,**31**:2008-2014

Preparation and Characterization of Monodispersed and Water-Soluble Gold Nano-Clusters

ZHANG Ming, WANG Shuai-Shuai,
ZHU Han, DU Ming-Liang

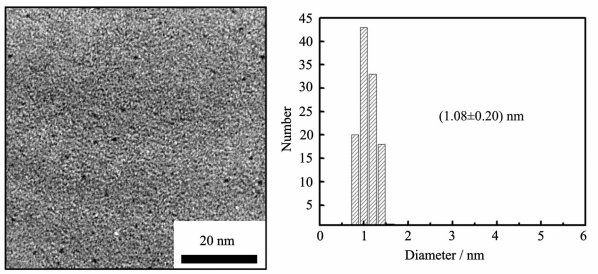

Monodispersed water-soluble gold nano-clusters were prepared with size of about 10.2 nm and the possible chemical formula of the synthesized gold nano-clusters was determined as $[Au_{38}(MSA\ Na)_{26}]$ or $[Au_{39}(MSA\ Na)_{27}]$.

DOI:10.11862/CJIC.2015.222
Chinese J. Inorg. Chem., **2015**,**31**:2015-2020

Adsorption of Nonionic Surfactant NP-40 on Micron/Nano Calcium Oxalate Monohydrate and Dihydrate Crystals

WEN Xiao-Ling, GAN Qiong-Zhi,
OUYANG Jian-Ming

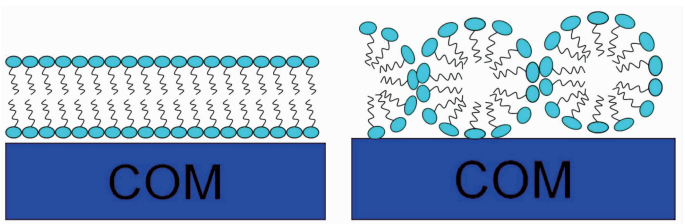

The interactions between the hydrophobic alkyl chains of the additional NP-40 and the exposed alkyl chains of the NP-40 adsorbed on the surface of COM formed a bilayer or micelles.

DOI:10.11862/CJIC.2015.266
Chinese J. Inorg. Chem., **2015**,**31**:2021-2029

Preparation and Electrochemical Performance of Sulfur/Mesoporous Carbon Composites as Cathodes for Lithium-Sulfur Batteries

XU Jing-Jing, LI Bin, LI Song-Mei,
LIU Jian-Hua, YU Mei

DOI:10.11862/CJIC.2015.223
Chinese J. Inorg. Chem., **2015**,**31**:2030-2036

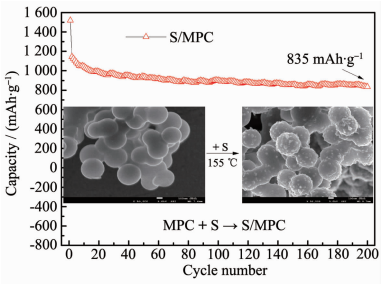

Sulfur/mesoporous carbon composites were achieved by melt infiltration of sulfur into mesoporous carbon which was prepared by template method. When the composites were applied as cathode material for lithium sulfur, the initial discharge specific capacity is as high as 1 519 mAh·g^{-1}, and can remain 835 mAh·g^{-1} even after 200 cycles.

$PW_{11}Cu/TiO_2$ Film Photocatalyst: Preparation and Visible Photocatalytic Performance

ZOU Xiao-Mei, CHEN Qi-Sheng,
KE Xiao-Xue, LEI Qin, ZHAO Zi-Ming,
LIU Xi-Long, CHEN Yan, HUA Ying-Jie,
WANG Chong-Tai

DOI:10.11862/CJIC.2015.232
Chinese J. Inorg. Chem., **2015**,**31**:2037-2043

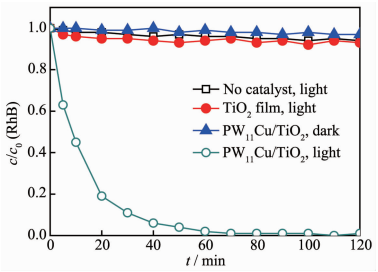

The visible photocatalytic degradation of RhB shows that the visible photocatalyst $PW_{11}Cu/TiO_2$ has a high photocatalytic activity.

Syntheses, Crystal Structures and Biological Activities of Bis(tricyclohexyltin)dicarboxylates with Macrocyclic Building 2D Network

KUANG Dai-Zhi, ZHU Xiao-Ming,
FENG Yong-Lan, ZHANG Fu-Xing,
YU Jiang-Xi, JIANG Wu-Jiu,
TAN Yu-Xing, ZHANG Zhi-Jian

DOI:10.11862/CJIC.2015.268
Chinese J. Inorg. Chem., **2015**,**31**:2044-2050

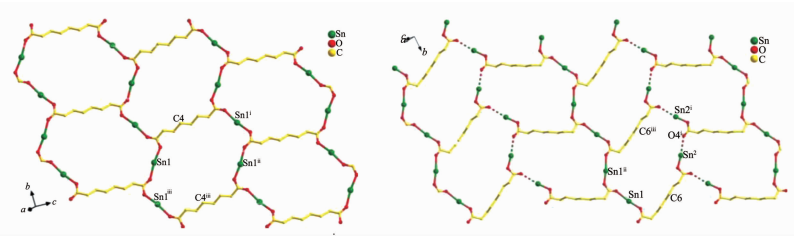

Two complexes respectively formed 30-membered and 32-membered macrocyclic tetratin species of 2D network structure, the complexes exhibited strong in vitro anti-tumor activity against five human tumor cell lines, Colo205, HepG2, MCF-7, Hela and NCI-H460.

Syntheses, Crystal Structures and Luminescent Properties of Two Cu(Ⅱ) Complexes with 2-(2-Pyridyl)imidazole Derivatives (English)

FAN Yan, QU Zhi-Rong, JIN Xiao-Fei,
GUO Yan-Hong, WANG Zuo-Xiang

DOI:10.11862/CJIC.2015.262
Chinese J. Inorg. Chem., **2015**,**31**:2051-2058

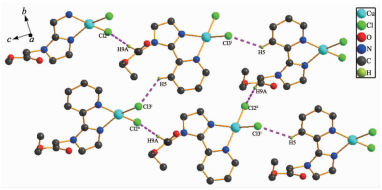

Two complexes, $[Cu(DMPM)_2(Bz)][Cu(DMPM)(Bz)_3]\cdot H_2O$ (**1**) and $[Cu(PMA)Cl_2]$ (**2**) (DMPM =4,5-dimethyl-2-(2-pyridyl) imidazole, PMA=ethyl [2-(2-pyridyl)imidazole-1-yl)]acetate, Bz =benzoate anion) were synthesized and characterized. Complex **2** assembles into a 2D layer structure by the intermolecular hydrogen bonding interactions. It shows high thermal stability and relatively strong fluorescence.

Syntheses, Crystal Structures and Properties of Three Transition Metal Coordination Compounds Based on 2,2′-Bipyridine-3,3′,6,6′-tetracarboxylic Acid (English)

BING Ying-Ying, WU Zhen-Ting, HU Ming

DOI:10.11862/CJIC.2015.264
Chinese J. Inorg. Chem., **2015**,**31**:2059-2064

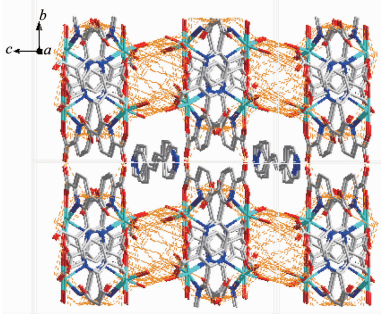

Three transition metal compounds based on 2,2′-bipyridine-3,3′,6,6′-tetracarboxylic acid have been obtained, which exhibit the different three-dimensional supramolecular architectures by strong hydrogen-bonding interactions.

Syntheses, Crystal Structures and Fluorescence Properties of Two Metal-Organic Coordination Polymers Derived from Rigid Bis(1,2,4-triazolyl) and Aromatic Carboxylic Acid Ligands (English)

WANG Xiao-Xiao, LIU Yong-Guang,
GE Ming, CUI Guang-Hua

DOI:10.11862/CJIC.2015.273
Chinese J. Inorg. Chem., **2015**,**31**:2065-2072

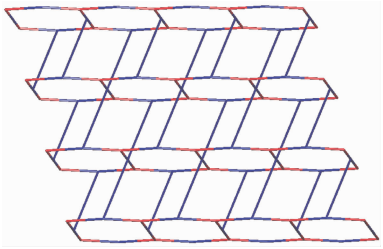

Two coordination polymers $[Co_{1.5}(btb)_2(nbta)(H_2O)_2]_n$ (**1**), and $[Cd(btb)_{0.5}(nph)(H_2O)]_n$ (**2**) have been synthesized by 4,4′-bis(1,2,4-triazolyl-1-yl)-biphenyl (btb) with different carboxylic acids as co-ligand. The structural analyses show that **1** display a 2D (3,4)-connected 3,4L90 network. Complex **2** is a 3D (3,4,4)-connected sqc69 network with the Schläfli symbol of $(4.8^2)_2$ $(4^2.8^2.10^2)(8.10^4.12)$.

Crystal Structures and Properties of Zn(Ⅱ)/Cd(Ⅱ) Coordination Polymers Based on Semirigid Tetrahedral Quadridentate Ligand (English)

TANG Wen-Yuan, REN Shi-Bin,
ZHU Dong-Dong, HAN De-Man,
ZHOU Xin-Hui

DOI:10.11862/CJIC.2015.229
Chinese J. Inorg. Chem., **2015**,**31**:2073-2078

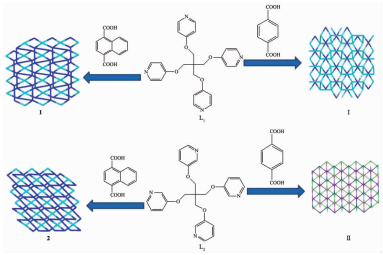

The comparation of their topological structure shows that the effect of steric hindrance of an auxiliary linker will strongly affect the structural diversity of CPs.

Synthesis and Characterization of Some Ferrocenylphenylimine Compounds (English)

Ikhile Monisola I, Ngila J Catherine

DOI:10.11862/CJIC.2015.272
Chinese J. Inorg. Chem., **2015**,**31**:2079-2088

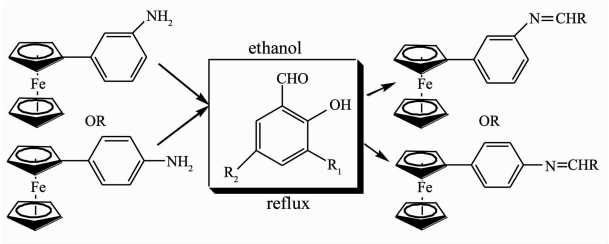

3-Ferrocenyl aniline and 4-ferrocenyl aniline were reacted with aromatic aldehyde in ethanol solution under reflux to produce 3-ferrocenyl phenyl imine and 4-ferrocenyl phenyl imine, respectively.

Syntheses and Characterization of Two Luminescent Silver (Ⅰ) Complexes Based on Mixed Phosphine Ligands (English)

ZHANG Yan-Ru, WANG Meng-Qin,
CUI Yang-Zhe, LIU Min, LI Zhong-Feng,
JIN Qiong-Hua

DOI:10.11862/CJIC.2015.274
Chinese J. Inorg. Chem., **2015**,**31**:2089-2094

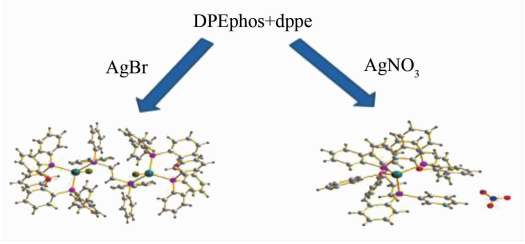

Complex **1** is comprised of AgBr, DPEphos and dppe (DPEphos =bis [2-(diphenylphosphino)phenyl]ether, dppe=bis(diphenylphosphino)ethane) in 2:2:1 molar ratio generating a binuclear complex. The dppe ligand bridges two Ag atoms through two P atoms. While, complex **2** is obtained by the reactions of $AgNO_3$, DPEphos and dppe in 1:1:1 molar ratio generating a sample mono-nuclear complex.